

# **Well-Defined Copper-Based Nanocatalysts for Selective Electrochemical Reduction of CO<sub>2</sub> to Ethylene and Ethanol**

Ludovic Zaza <sup>1</sup>, Kevin Rossi <sup>1</sup>, Raffaella Buonsanti <sup>1</sup>\*

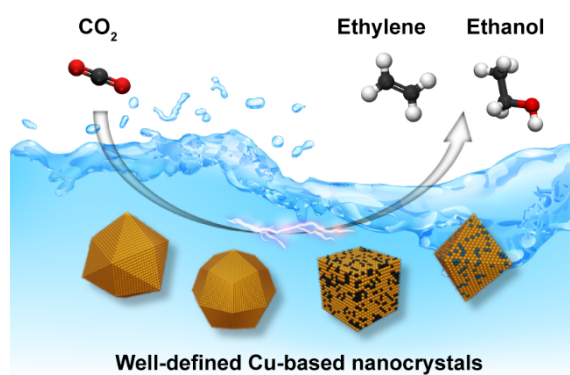
<sup>1</sup>Laboratory of Nanochemistry for Energy (LNCE), Department of Chemical Sciences and Engineering, École Polytechnique Fédérale de Lausanne, CH-1950 Sion, Switzerland.

\* Correspondence to: [raffaella.buonsanti@epfl.ch](mailto:raffaella.buonsanti@epfl.ch)

## ABSTRACT

The electrochemical CO<sub>2</sub> reduction reaction (CO<sub>2</sub>RR) holds the promise to revolutionize the chemical industry by producing value-added chemicals and fuels from CO<sub>2</sub> and water while storing renewable energy. However, catalyst design still remains one of the major hurdles in the field. This Perspective discusses the current and future contribution of well-defined nanocatalysts to improving the CO<sub>2</sub>RR selectivity towards C<sub>2</sub> products, particularly ethylene and ethanol. In this regard, the shape and size selectivity dependence of single metal copper nanocrystals is briefly reviewed and linked to single crystal studies. Representative studies on Cu-based bimetallic nanocrystals are discussed to highlight the importance of composition and distribution of the metals for selectivity. Finally, a vision on design strategies of shape and composition for the next generation of CO<sub>2</sub>RR nanocatalysts is proposed.

### Table of Contents (TOC) Graphic:



The electrochemical CO<sub>2</sub> reduction reaction (CO<sub>2</sub>RR) is a promising approach to mitigate the effects of anthropogenic atmospheric CO<sub>2</sub> release by recycling it into valuable chemicals and fuels. As electricity from renewable sources provides the energy for this conversion, CO<sub>2</sub>RR enables the storage of renewable energy into chemical bonds, which adds value to this process compared to thermal CO<sub>2</sub> conversion. CO<sub>2</sub>RR products include C<sub>1</sub> compounds, such as carbon monoxide (CO), formate (HCOO<sup>-</sup>), methane (CH<sub>4</sub>), C<sub>2</sub> compounds, such as ethylene (C<sub>2</sub>H<sub>4</sub>) and ethanol (C<sub>2</sub>H<sub>5</sub>OH), and C<sub>2+</sub>, such as propanol (C<sub>3</sub>H<sub>7</sub>OH). Among them, ethylene and ethanol are desirable targets because of their higher energy density and their economic potential.<sup>1</sup>

CO<sub>2</sub>RR requires a catalyst to activate the stable CO<sub>2</sub> molecule and to direct product selectivity. Among different materials, copper has the unique capacity to catalyze C-C coupling and, thus, to form C<sub>2</sub> and C<sub>2+</sub> products.<sup>1-7</sup> This property can be understood in light of the Sabatier principle, which states that the optimal binding energy towards crucial reaction intermediates must be neither “too strong” nor “too weak” for an ideal catalyst. If intermediate molecules bind too strongly to the surface, they would poison the catalyst. If they bind too weakly, the intermediates would be released from the active sites prematurely, before entering in the next step of the reaction. Copper possesses an optimal binding energy towards crucial CO<sub>2</sub>RR intermediates, including \*H, \*COOH, \*CO and \*CHO, which account for its catalytic behavior.<sup>6,7</sup>

Unfortunately, polycrystalline Cu foil is unselective as it forms up to 16 different products.<sup>5</sup> Pioneering studies on single crystals from Hori and co-workers have revealed the structural dependence of CO<sub>2</sub>RR, which can render Cu more selective.<sup>3,4</sup> For example, Cu (100) and Cu (111) surfaces selectively produce ethylene and methane, respectively.<sup>4</sup> However, while single crystal electrodes are crucial to develop a fundamental understanding in electrocatalysis, they cannot be integrated into an actual catalytic reactor.

In addition to structural modification, the incorporation of a second metal to Cu has emerged as a valid strategy to steer the selectivity towards different products.<sup>8-15</sup> However, contrasting results in terms of major CO<sub>2</sub>RR product exist in the literature for catalysts with similar composition.<sup>11-15</sup> This inconsistency might arise from differences in structure and local arrangement of the bimetallic catalysts, which suggest that these features are as important as composition, thus their impact on the catalytic behavior must be studied.

Well-defined nanocatalysts are ideal model systems to investigate structure-performance relationships in electrocatalysis.<sup>16,17</sup> Indeed, their well-defined sizes and shapes aid to translate finding from single crystals into a larger variety of testing conditions along with revealing beneficial nanoscale effects.<sup>16,18</sup> Furthermore, their structural and compositional tunability is ideal to gain insight into and optimize the catalytic performance of bimetallic catalysts.<sup>16,17</sup> Among different techniques, colloidal chemistry provides the opportunity to synthesize nanocrystals (NCs) with a tunability which other approaches cannot match.<sup>16</sup> Additionally, these colloidal NCs are produced as inks, which are easily processable for integration in different types of electrochemical reactors.<sup>16,17</sup>

In this Perspective, we discuss the design strategies of Cu-based NCs to steer the CO<sub>2</sub>RR selectivity towards C<sub>2</sub> products, particularly ethylene and ethanol. First, we highlight the advances in CO<sub>2</sub>RR selectivity made by tuning the shape and the size of Cu NCs with a link to single crystal studies. We then discuss selected examples of bimetallic NCs which highlight the contribution of compositionally well-defined NCs to understand structure-property relationship in more complex catalysts. For both aspects, we propose strategies to further advance the current state of the art in catalyst design for CO<sub>2</sub>RR.

## DIRECTING CO<sub>2</sub>RR SELECTIVITY BY TAILORING THE SIZE AND SHAPE OF COPPER NANOCRYSTALS

The NC shape dictates the crystallographic facets exposed on the surface. For face-centered cubic metals like copper, the surface energy,  $\gamma$ , of the different facets (i.e.  $\gamma_{\{111\}} < \gamma_{\{100\}} < \gamma_{\{110\}}$ ) results in the formation of a truncated octahedron, enclosed by  $\{100\}$  and  $\{111\}$  facets, as the thermodynamically favorable shape.<sup>19</sup> Truncated octahedra are normally regarded as “spheres” because they appear very similar to a spherical particle in electron microscopy images. Different shapes can be obtained by using ligands which selectively bind to certain facets, thus modifying their surface energies.<sup>19</sup> Judicious modifications of the reaction conditions provide an additional mean to target metastable shapes by acting on the solution chemical potential.<sup>20</sup> As a result, a catalogue of several shapes is currently available for single metal Cu NCs, synthesized in one step and without seeding. These shapes include spheres<sup>21,22</sup>, tetrahedra<sup>20</sup>, octahedra<sup>23,24</sup> and star-shaped decahedra<sup>25</sup>, which all expose mostly  $\{111\}$  facets, cubes<sup>20,21,26</sup>, which expose mostly  $\{100\}$  facets, and nanorods, which possess a  $\{111\}$  pentagonal cross-section and  $\{100\}$  side faces<sup>27</sup>. Among these shaped NCs, spheres, octahedra, star-shaped decahedra, cubes and nanorods were tested as CO<sub>2</sub>RR catalysts.<sup>22,24,25-29</sup> In the absence of grain boundaries effects<sup>25,27</sup>, the major reaction products followed the same structural dependent trend discovered in single crystal experiments.<sup>22,24,26,28,29</sup> Namely, the Cu octahedra evolved methane and the Cu cubes yielded ethylene as the major products. The Cu spheres were not found particularly selective towards any product, which indeed resembles the behavior of the polycrystalline copper foil.

In addition to shape, size greatly affects the performance of Cu NCs during the CO<sub>2</sub>RR. For instance, CO and H<sub>2</sub> production drastically increased at the expense of hydrocarbons for Cu

spheres with diameter < 5 nm compared to bigger sizes.<sup>22</sup> Cu cubes with edge length of 44 nm possessed a greater selectivity for ethylene compared to smaller (edge length of 24 nm) and bigger (edge length of 63 nm) cubes.<sup>26</sup> Specifically, their faradaic efficiency (FE, which indicates the number of electrons converted into products) for ethylene was around 40% at -1.1 V<sub>RHE</sub> (RHE = reversible hydrogen electrode) compared to 9% and 25% for the smaller and bigger cubes, respectively. Cu octahedra with edge length of 75 nm produced more methane than the bigger sized 150 nm and 310 nm NCs.<sup>24</sup> Their FE for methane was 55% at -1.25 V<sub>RHE</sub> compared to around 40% for the medium size, while the bigger octahedra produced mostly hydrogen under the same conditions. The result on the spheres indicates that increasing the number of certain undercoordinated sites eventually favors the hydrogen evolution reaction (HER), which competes with CO<sub>2</sub>RR. The size-dependent behavior of the cubes and of the octahedra underscores the importance of the face/edge ratio to optimize product selectivity. In particular, the {100}/{110} ratio modulates the selectivity towards ethylene. DFT calculations revealed that the activation energy for the \*CO-\*COH coupling to form C<sub>2</sub> products is indeed reduced at {100}/{110} step sites compared to the \*CO-\*CO dimerization and \*CO-\*COH coupling on {100} surfaces.<sup>30</sup> Similarly, the amount of {111}/{110} and {111}/{100} step sites correlates with methane formation as the ratio between these two facets decreases as the octahedra get smaller. Altogether, studies on well-defined NCs indicate that an optimal size exists for nanocatalysts to maximize positive synergistic effects arising at the interface between different facets, a lesson learned which goes beyond the insight provided by single crystals (**Figure 1**).

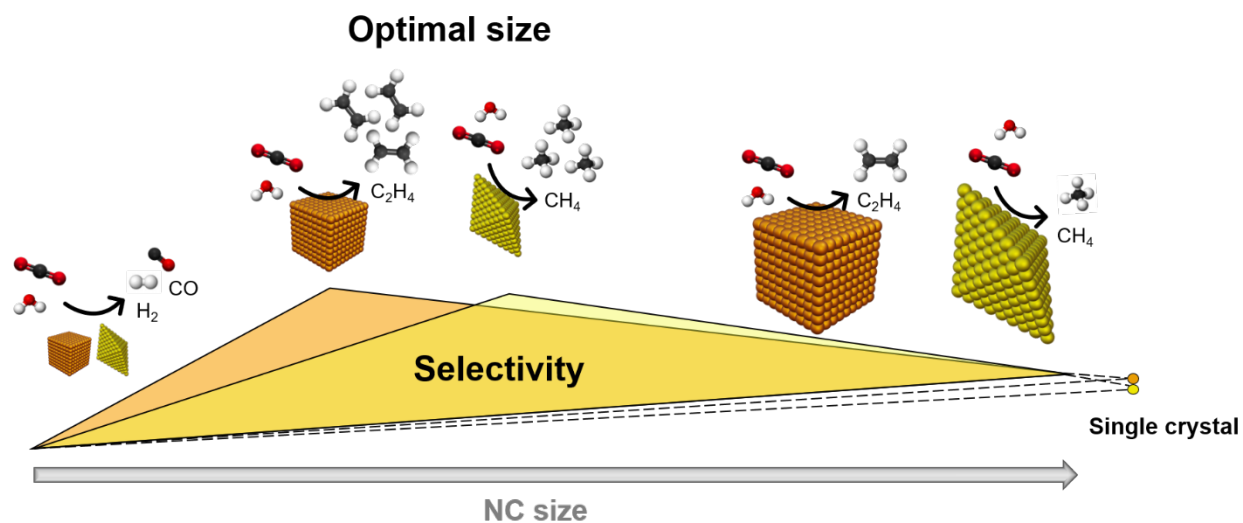


**Figure 1. Schematic illustration of size- and shape- dependent behavior of Cu NCs in CO<sub>2</sub>RR.**

An optimal NC size exist, which maximizes synergistic effects arising at the face/edge interface and thus, the selectivity towards certain products. Above this size, the NC catalytic behavior resembles more closely that of a single crystal which exposes the surface corresponding to the major facets enclosing the NCs. When the size decreases below the optimum, the density of undercoordinated sites at corners, steps, and kinks increases, which eventually promotes 2 electrons reducing pathways, such as HER and CO.

It is worthwhile to highlight that the studies on Cu NCs have been so far limited to those NCs enclosed by the most stable low-index facets {100}, {110} and {111}. However, single crystal studies suggest that the high-index Cu(511), Cu(711), Cu(911), Cu(11,1,1), Cu(310), Cu(510), Cu(610), and Cu(810) facets possess an even greater ethylene-to-methane ratio and overall C<sub>2</sub> selectivity than the Cu(100) facet.<sup>4,31</sup> If the focus shifts from hydrocarbons to alcohols, Cu(310), Cu(510), Cu(610) and Cu(810) have higher FE for ethanol compared to the Cu (100) surface.<sup>4,31</sup> These high-index facets (HIF) can be visualized as a combination of terraces and steps of low-index facets, written as  $n(h_1k_1l_1) \times (h_s k_s l_s)$ , where the number  $n$  is the width of  $(h_1k_1l_1)$  terraces with

monoatomic ( $h_s k_s l_s$ ) steps.<sup>32</sup> For instance,  $\{2n-1,1,1\}$  and  $\{n,1,0\}$  HIF can be referred as  $n\{100\} \times \{111\}$  and  $n\{100\} \times \{110\}$ , respectively. The face/edge interfaces in cubes and octahedra mimic some of these structural motifs, for example the  $\{100\}/\{110\}$  interface resembles the  $\{2n-1,1,1\}$  structure. As just discussed, decreasing the NC size increases their contribution to the overall selectivity. However, this effect can be exploited only until the point where the unfavorable contribution of the HER-selective kinks and corners starts to dominate on the catalytic behavior. HIF NCs would overcome this limitation by maximizing the contribution of active sites, independently from the NC size (**Figure 2A**). Furthermore, interesting trends might emerge from the combinations of different HIF within the same NCs (**Figure 2B**), which are not accessible by single crystal studies. Thus, HIF NCs become a platform to uncover potential synergistic effects between different facets and eventually improve selectivity beyond what is predicted.

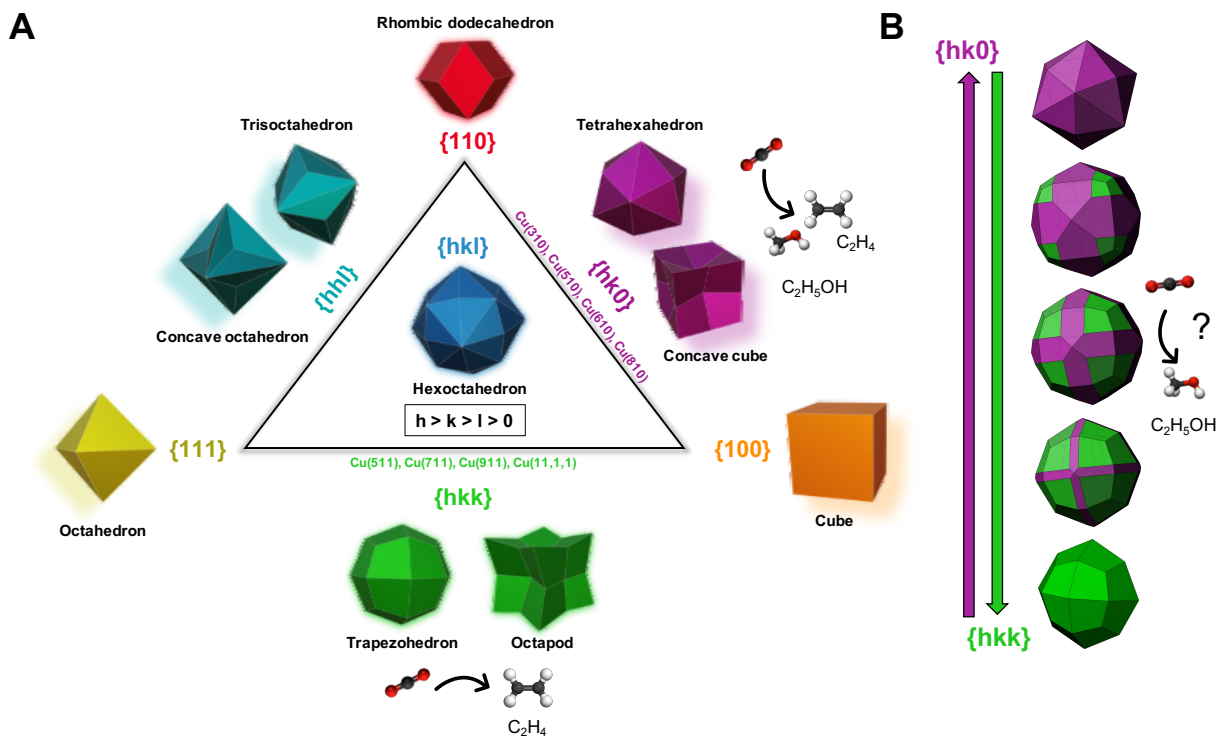




**Figure 2. Schematic illustrations of HIF Cu NCs as selective CO<sub>2</sub>RR catalysts towards C<sub>2</sub> products.** (A) Examples of convex and concave geometric figures enclosed by high crystallographic index facets. Cu facets showing enhanced C<sub>2</sub> selectivity compared to Cu {100} are highlighted accordingly. (B) Example of HIF NCs combining features from trapezohedron (enclosed by {hkk}, in green) and tetrahexahedron (enclosed by {hk0}, in purple). A higher selectivity towards ethanol is proposed since n(100)x(110) step sites were shown to favor ethanol vs ethylene formation.<sup>4,31</sup>

## **DIRECTING CO<sub>2</sub>RR SELECTIVITY BY STRUCTURAL AND COMPOSITIONAL TUNING OF CU-BASED BIMETALLIC NANOCRYSTALS**

The two main driving forces for selectivity in bimetallic catalysts are the changes in the binding energy of intermediates, which occur via electronic and geometric effects, and the supply of reaction intermediates to copper (e.g. CO), which is referred to as tandem catalysis.<sup>8-15</sup> These effects are often convoluted, which makes it difficult to gain insight into the behavior of these catalysts and, thus, to develop accurate predictions.<sup>8-15</sup> As a matter of fact, a rational selection of the element that, added to copper, leads to the desired product is still lacking. While CO<sub>2</sub>RR selectivity trends for bimetallic alloyed catalysts have been predicted based on the adsorption energy for \*H and \*CO, these studies don't provide information on the actual products.<sup>8,9,33,34</sup>

If we focus on examples where a CO-producing metal, such as Ag, Pd, Zn, is added to Cu, the overall promotion of C<sub>2</sub> products has been consistently demonstrated, yet contrasting results in terms of major CO<sub>2</sub>RR product (e.g. hydrocarbons vs oxygenated products) exist in the literature.<sup>11-15</sup> As aforementioned, this inconsistency might arise from comparing on the same footing catalysts solely on the basis of their composition notwithstanding that they possess

different sizes, morphologies, stoichiometries, and chemical arrangements. Studies on well-defined NCs clarify further this observation.

In one example, CuPd nanocatalysts were synthesized as random alloys, intermetallics (ordered alloys) and phase-separated bimetallics.<sup>35</sup> The phase-separated catalyst exhibited the highest FE for C<sub>2</sub> products, up to 62% versus only 5% measured for the ordered one at -0.8V<sub>RHE</sub>. At around the same potential, the ordered and disordered bimetallics produced methane, with FE close to 8%; instead, methane was at the detection limit for the phase-separated CuPd. All catalysts possessed the same CO FE of ~40% at cathodic potentials of -0.3V<sub>RHE</sub>. However, at the more negative potentials which evolve C<sub>2</sub> products, the ordered and the phase-separated CuPd exhibited the highest and the lowest CO FE. Altogether these data suggest that for the CuPd nanocatalysts: i) CO is an important intermediate for C<sub>2</sub> chemicals; ii) phase-segregation is beneficial to convert CO to C<sub>2</sub> chemicals; iii) more homogeneous mixing patterns favor the production of methane. The stabilization of the \*CHO intermediate via the presence of an oxophilic metal in the vicinity of copper provides a reasonable explanation for this last observation.

A study on Ag-Cu nanodimers, where well-defined spherical domain of Ag and Cu share an interface, has then evidenced the importance of an actual interface between the two metals versus having simply physical mixing to boost C-C coupling and ethylene selectivity in tandem catalysis.<sup>36</sup> First of all, the nanodimers showed a significant enhancement in selectivity toward ethylene compared to Cu NCs of similar size and shape, with FE improving from 12% to ~40% at -1.1 V<sub>RHE</sub>. The nanodimers possessed also double FE towards ethylene compared to a physical mixture of Ag and Cu NCs. The latter had a FE for ethylene of ~20% at -1.1 V<sub>RHE</sub>, which is still higher than bare Cu NCs because of tandem effects. The coexistence of electronic effects and of tandem catalysis explained the improved performance of the nanodimers towards ethylene

production. Indeed, an interfacial charge transfer from Cu to Ag was proved, which leaves a partial positive charge on the Cu domain. This partial positive charge stabilizes adsorbed \*CO and promotes C-C coupling. The Cu domain size was then tuned and the nanodimers including the middle size domain of around 25 nm were optimal for C-C coupling, which highlighted the existence of a delicate balance between the tandem effect and the extension of the interface to maximize the faradaic efficiency towards ethylene.

A recent study on alloyed CuZn NCs has highlight that the percentage of the second metal to Cu impact the mechanism which direct selectivity and, thus, the final CO<sub>2</sub>RR product.<sup>37</sup> Specifically, the CuZn NCs with 5% Zn content were selective for methane, with a maximum FE of 52% at -1.4 V<sub>RHE</sub>. The CuZn NCs with 19% Zn were selective for ethanol, with a maximum FE of 39% at -1.3 V<sub>RHE</sub>. Furthermore, these catalysts with higher Zn content also produced more CO. Theory showed that isolated Zn atoms, which are more likely to exist in the CuZn NCs with 5% Zn, modify the electronic properties of copper so to stabilize the methane-producing \*CHO intermediate, similarly to the Pd case. As the number of neighboring Zn atoms increases with the Zn content, the propensity of the CuZn catalysts to release CO increases. The higher concentration of local CO enhances C-C coupling, which is a typical tandem effect. Thus, tandem and electronic effects might be called out again to explain the ethanol selectivity of the CuZn NCs with higher Zn content.

These selected examples highlight a general trend in bimetallic catalysts including a CO-producing domain (**Figure 3**). Specifically, that tandem mechanism dominates when phase segregation occurs. Instead, electronic effects prevail in systems with a more homogeneous distribution of the two elements.

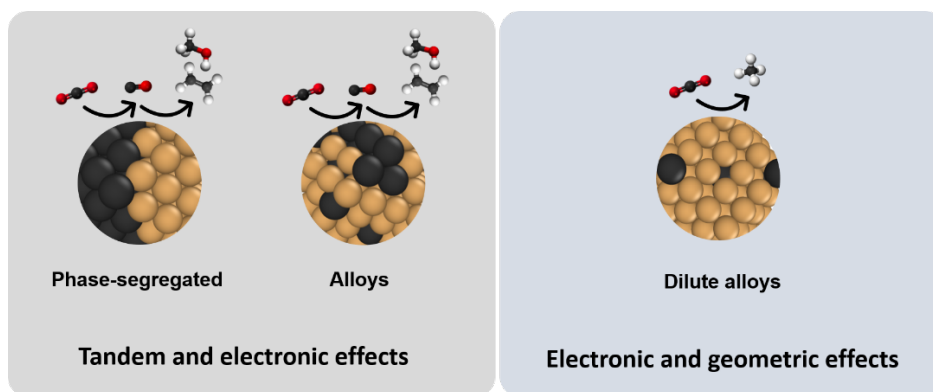


**Figure 3. Schematic illustration of selectivity changes in bimetallic Cu-based NCs including a CO-generating element.** The presence of neighboring atoms of the CO-generating metals in phase-segregating catalysts and random alloys induces tandem effects which promote  $C_2$  products in convolution with electronic effect. Instead, electronic and geometric effects will dictate selectivity in bimetallic NCs with a more homogeneous elemental distribution, such as dilute alloys. For example, the stabilization of the  $^*CHO$  intermediate resulting from the addition of an element more oxophilic than copper will generate methane as the major  $CO_2RR$  product.

This observation suggests one possible strategy to advance the current state of the art in predicting the catalytic behavior of bimetallic catalysts for  $CO_2RR$ . Theorists and experimentalists should work together on model systems, which can help to deconvolute the interplay between catalyst structure, composition, and elemental arrangement. For example, dilute alloyed NCs emerge as an ideal candidate to isolate and focus on the geometric and electronic structure effects only. Once a class of model systems is established, two descriptors,  $D_1$  and  $D_2$ , whose magnitude is predicted to correlate with a certain product, should be selected. For example,  $D_1$  could be the formation energy of  $^*COH$  via the protonation of adsorbed  $^*CO$  for the production of  $C_1$  products and  $D_2$  could be  $^*CO$  desorption energy for  $C_2$  products, if the goal is to discern  $C_2$  vs  $C_1$  selectivity.<sup>38,39</sup> The changes in  $D_1$  and  $D_2$  should then be screened for different metal dopants in copper (**Figure**

4). After this, theoretical prediction should identify a number of systems with diverse CO<sub>2</sub>RR selectivity. The result of this prediction should be then validated by experiment, to verify whether the employed descriptors are reliable in their use. The knowledge acquired from these diluted alloys should then be used to move on to systematic studies which compare alloys with different compositions, nanodimers and physical mixtures of nanocatalysts with same size. Shape control should then be explored next to study structural effects in bimetallic, interesting but even less studied so far.<sup>34</sup>

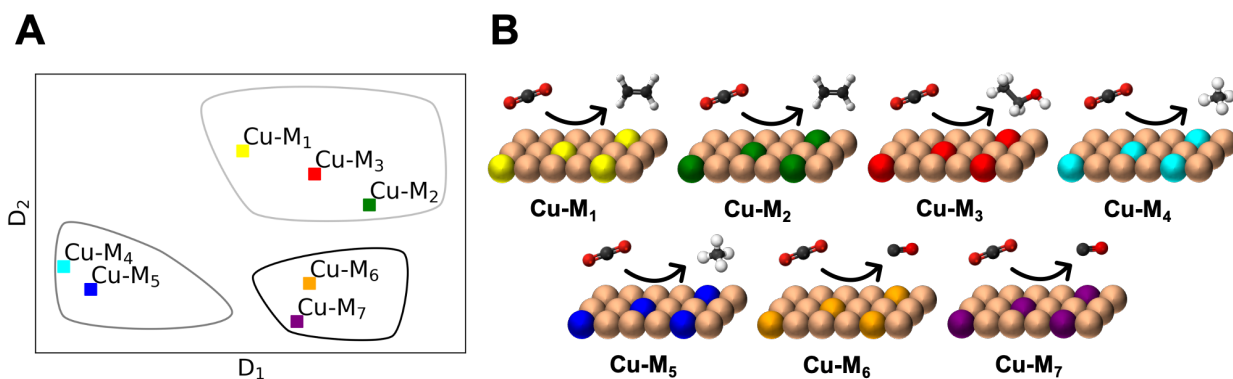


**Figure 4. Schematic illustration of a combined theory-experimental strategy to predict product selectivity in Cu-based bimetallic catalysts.** (A) Classification of different Cu-M<sub>x</sub> dilute alloys based upon abstract descriptors. (B) Schematic illustration of different dilute alloys and the corresponding majority products they are selective for, as per correctly classified by the graph in A.

## SUMMARY

The design of selective CO<sub>2</sub>RR electrocatalysts still remains one of the major hurdles in the field. This Perspective has emphasized the contribution of well-defined mono- and bimetallic Cu-based NCs to achieve selective CO<sub>2</sub>RR by establishing crucial structure-composition-performance relationships. Future directions were also proposed. In particular, HIF Cu NCs for enhanced ethylene selectivity and dilute Cu-based alloys as platforms to isolate geometric and electronic effects induced by a second metal and to move towards a more rational design of bimetallic catalysts.

Synthetic challenges for HIF Cu NCs exist as their formation requires the stabilization of high energy surfaces. Nevertheless, the nanochemistry community should be able to address those in the upcoming years, as numerous examples of HIF noble metal NCs exist in the literature.<sup>40,41</sup> As for the dilute alloyed NCs, some of the strategies developed for doping of chalcogenide and oxide NCs could be revised to specifically target metallic NCs.<sup>42</sup>

Certainly, changes under operating conditions are not easy to predict but should be monitored. Eventually, strategies including a thin layer of graphene oxide could be implemented to avoid reconstruction of the HIF NCs or the preferential dissolution of one element in the bimetallics.<sup>27</sup> Furthermore, the probability of dopant atoms aggregating and clustering in the dilute alloys is expected to be low even during operation, if the assumption that entropy controls the chemical ordering in these systems is valid.

Finally, while the focus of this Perspective was catalyst design, other important factors, which include the pH and cations in the electrolyte, the electrochemical reactor, the membrane, the catalyst microenvironment, will also play a critical role in reaching the desired selectivity during CO<sub>2</sub>RR and should be considered when optimizing the whole system.<sup>43-47</sup>

## AUTHOR INFORMATION

### Corresponding Author

Email: [raffaella.buonsanti@epfl.ch](mailto:raffaella.buonsanti@epfl.ch)

### Notes

The authors declare no competing financial interest.

### Biographies

**Ludovic Zaza** obtained his Master degree in Chemical Engineering and Biotechnology from the Ecole Polytechnique Fédérale de Lausanne (Switzerland) in 2021. He joined Prof. Buonsanti's group in October 2021 as a PhD candidate. His research focuses on the development of new methods for the synthesis of Cu-based nanocrystals.

**Kevin Rossi** obtained his PhD in Physics from King's College London in 2019 under the supervision of Prof. Baletto. He then undertook a Postdoc researcher role in Prof. Ceriotti's lab at the Ecole Polytechnique Fédérale de Lausanne (Switzerland) between 2018 and 2020. Since September 2020 he has been a Marie Curie Sklodowska Fellow hosted in Prof. Buonsanti's lab. His research focuses on the use of numerical and data-driven methods to address problems of relevance to green energy and green chemistry.

**Raffaella Buonsanti** received her master degree in Chemistry from the University of Bari. After been awarded her PhD in Nanochemistry from the University of Salento working at the National Nanotechnology Laboratory, she spent almost six years at Lawrence Berkeley National Laboratory, first as a postdoctoral researcher and project scientist at the Molecular Foundry, later as a staff scientist at the Joint Center of Artificial Photosynthesis. Since 2015, she is a tenure-track Assistant Professor in the Institute of Chemical Sciences and Engineering at the École Polytechnique Fédérale de Lausanne. She leads a multidisciplinary program which spans from materials chemistry and nanoscience to catalysis, electrochemistry and sustainability. Her team is interested in the synthetic development of nanocrystals and their use as electrocatalysts to drive the conversion of small molecule and as materials to advance different energy technologies.

## **ACKNOWLEDGEMENTS**

KR acknowledges the H2020 Marie Curie Individual Fellowship grants NANOCO2RE with agreement number 890414. This publication was created as part of NCCR Catalysis, a National Centre of Competence in Research funded by the Swiss National Science Foundation.



## REFERENCES

1. Nitopi, S.; Bertheussen, E.; Scott, S. B.; Liu, X.; Engstfeld, A. K.; Horch, S.; Seger, B.; Stephens, I. E. L.; Chan, K.; Hahn, C.; et al. Progress and Perspectives of Electrochemical CO<sub>2</sub> Reduction on Copper in Aqueous Electrolyte. *Chem. Rev.* **2019**, *119*(12), 7610-7672. DOI: 10.1021/acs.chemrev.8b00705
2. Larrazábal, G. O.; Martín, A. J.; Pérez-Ramírez, J. Building Blocks for High Performance in Electrocatalytic CO<sub>2</sub> Reduction: Materials, Optimization Strategies, and Device Engineering. *J. Phys. Chem. Lett.* **2017**, *8*(16), 3933-3944. DOI: 10.1021/acs.jpcllett.7b01380
3. Hori, Y.; Wakebe, H.; Tsukamoto, T.; Koga, O. Electrocatalytic Process of CO Selectivity in Electrochemical Reduction of CO<sub>2</sub> at Metal Electrodes in Aqueous Media. *Electrochim. Acta* **1994**, *39*(11-12), 1833-1839. DOI: 10.1016/0013-4686(94)85172-7
4. Hori, Y.; Takahashi, I.; Koga, O.; Hoshi, N. Electrochemical Reduction of Carbon Dioxide at Various Series of Copper Single Crystal Electrodes. *J. Mol. Catal. A: Chem.* **2003**, *199*(1-2), 39-47. DOI: 10.1016/S1381-1169(03)00016-5
5. Kuhl, K. P.; Cave, E. R.; Abram, D. N.; Jaramillo, T. F. New Insights into the Electrochemical Reduction of Carbon Dioxide on Metallic Copper Surfaces. *Energy Environ. Sci.* **2012**, *5*(5), 7050-7059. DOI: 10.1039/c2ee21234j
6. Liu, X.; Xiao, J.; Peng, H.; Hong, X.; Chan, K.; Nørskov, J. K. Understanding Trends in Electrochemical Carbon Dioxide Reduction Rates. *Nat. Commun.* **2017**, *8*(1), 15438. DOI: 10.1038/ncomms15438
7. Bagger, A.; Ju, W.; Varela, A. S.; Strasser, P.; Rossmeisl, J. Electrochemical CO<sub>2</sub> Reduction: A Classification Problem. *ChemPhysChem* **2017**, *18*(22), 3266-3273. DOI: 10.1002/cphc.201700736
8. Kim, C.; Dionigi, F.; Beermann, V.; Wang, X.; Möller, T.; Strasser, P. Alloy Nanocatalysts for the Electrochemical Oxygen Reduction (ORR) and the Direct Electrochemical Carbon Dioxide Reduction Reaction (CO<sub>2</sub>RR). *Adv. Mater.* **2019**, *31*(31), 1805617. DOI: 10.1002/adma.201805617
9. Vasileff, A.; Xu, C.; Jiao, Y.; Zheng, Y.; Qiao, S. Z. Surface and Interface Engineering in Copper-Based Bimetallic Materials for Selective CO<sub>2</sub> Electroreduction. *Chem* **2018**, *4*(8), 1809-1831. DOI: 10.1016/j.chempr.2018.05.001
10. Karapinar, D.; Creissen, C. E.; Rivera de la Cruz, J. G.; Schreiber, M. W.; Fontecave, M. Electrochemical CO<sub>2</sub> Reduction to Ethanol with Copper-Based Catalysts. *ACS Energy Lett.* **2021**, *6*(2), 694-706. DOI: 10.1021/acsenenergylett.0c02610
11. Ren, D.; Gao, J.; Pan, L.; Wang, Z.; Luo, J.; Zakeeruddin, S. M.; Hagfeldt, A.; Grätzel, M. Atomic Layer Deposition of ZnO on CuO Enables Selective and Efficient Electroreduction of Carbon Dioxide to Liquid Fuels. *Angew. Chem. Int. Ed.* **2019**, *58*(42), 15036-15040. DOI: 10.1002/anie.201909610
12. Ren, D.; Ang, B. S. H.; Yeo, B. S. Tuning the Selectivity of Carbon Dioxide Electroreduction toward Ethanol on Oxide-Derived Cu<sub>x</sub>Zn Catalysts. *ACS Catal.* **2016**, *6*(12), 8239-8247. DOI: 10.1021/acscatal.6b02162
13. Jeon, H. S.; Timoshenko, J.; Scholten, F.; Sinev, I.; Herzog, A.; Haase, F. T.; Roldan Cuenya, B. Operando Insight into the Correlation between the Structure and Composition of CuZn Nanoparticles and Their Selectivity for the Electrochemical CO<sub>2</sub> Reduction. *J. Am. Chem. Soc.* **2019**, *141*(50), 19879-19887. DOI: 10.1021/jacs.9b10709

14. Lum, Y.; Ager, J. W. Sequential Catalysis Controls Selectivity in Electrochemical CO<sub>2</sub> Reduction on Cu. *Energy Environ. Sci.* **2018**, *11*(10), 2935-2944. DOI: 10.1039/C8EE01501E
15. Clark, E. L.; Hahn, C.; Jaramillo, T. F.; Bell, A. T. (2017). Electrochemical CO<sub>2</sub> Reduction over Compressively Strained CuAg Surface Alloys with Enhanced Multi-Carbon Oxygenate Selectivity. *J. Am. Chem. Soc.* **2017**, *139*(44), 15848-15857. DOI: 10.1021/jacs.7b08607
16. Guntern, Y. T.; Okatenko, V.; Pankhurst, J.; Varandili, S. B.; Iyengar, P.; Koolen, C.; Stoian, D.; Vavra, J.; Buonsanti, R. Colloidal Nanocrystals as Electrocatalysts with Tunable Activity and Selectivity. *ACS Catal.* **2021**, *11*(3), 1248-1295. DOI: 10.1021/acscatal.0c04403
17. Shi, Y.; Lyu, Z.; Zhao, M.; Chen, R.; Nguyen, Q. N.; Xia, Y. Noble-Metal Nanocrystals with Controlled Shapes for Catalytic and Electrocatalytic Applications. *Chem. Rev.* **2020**, *121*(2), 649-735. DOI: 10.1021/acs.chemrev.0c00454
18. Koper, M. T. Structure Sensitivity and Nanoscale Effects in Electrocatalysis. *Nanoscale* **2011**, *3*(5), 2054-2073. DOI: 10.1039/C0NR00857E
19. Xia, Y.; Xiong, Y.; Lim, B.; Skrabalak, S. E. Shape-Controlled Synthesis of Metal Nanocrystals: Simple Chemistry Meets Complex Physics?. *Angew. Chem. Int. Ed.* **2009**, *48*(1), 60-103. DOI: 10.1002/anie.200802248
20. Strach, M.; Mantella, V.; Pankhurst, J. R.; Iyengar, P.; Loiudice, A.; Das, S.; Corminboeuf, C.; van Beek, W.; Buonsanti, R. Insights into Reaction Intermediates to Predict Synthetic Pathways for Shape-Controlled Metal Nanocrystals. *J. Am. Chem. Soc.* **2019**, *141*(41), 16312-16322. DOI: 10.1021/jacs.9b06267
21. Guo, H.; Chen, Y.; Cortie, M. B.; Liu, X.; Xie, Q.; Wang, X.; Peng, D. L. Shape-Selective Formation of Monodisperse Copper Nanospheres and Nanocubes via Disproportionation Reaction Route and Their Optical Properties. *J. Phys. Chem. C* **2014**, *118*(18), 9801-9808. DOI: 10.1021/jp5014187
22. Reske, R.; Mistry, H.; Behafarid, F.; Roldan Cuenya, B.; Strasser, P. Particle Size Effects in the Catalytic Electroreduction of CO<sub>2</sub> on Cu Nanoparticles *J. Am. Chem. Soc.* **2014**, *136* (19), 6978-6986. DOI: 10.1021/ja500328k
23. Lu, S.C.; Hsiao, M.C.; Yorulmaz, M.; Wang, L.Y.; Yang, P.Y.; Link, S.; Chang, W.S.; Tuan, H.Y. Single-Crystalline Copper Nano-Octahedra. *Chem. Mater.* **2015**, *27*(24), 8185-8188. DOI: 10.1021/acs.chemmater.5b03519
24. Iyengar, P.; Huang, J.; De Gregorio, G. L.; Gadiyar, C.; Buonsanti, R. Size Dependent Selectivity of Cu Nano-Octahedra Catalysts for the Electrochemical Reduction of CO<sub>2</sub> to CH<sub>4</sub>. *Chem. Commun.* **2019**, *55*(60), 8796-8799. DOI: 10.1039/C9CC02522G
25. Choi, C.; Cheng, T.; Flores Espinosa, M.; Fei, H.; Duan, X.; Goddard III, W. A.; Huang, Y. A Highly Active Star Decahedron Cu Nanocatalyst for Hydrocarbon Production at Low Overpotentials. *Adv. Mater.* **2019**, *31*(6), 1805405. DOI: 10.1002/adma.201805405
26. Loiudice, A.; Lobaccaro, P.; Kamali, E. A.; Thao, T.; Huang, B. H.; Ager, J. W.; Buonsanti, R. Tailoring Copper Nanocrystals towards C<sub>2</sub> Products in Electrochemical CO<sub>2</sub> Reduction. *Angew. Chem. Int. Ed.* **2016**, *55*(19), 5789-5792. DOI: 10.1002/anie.201601582
27. Li, Y.; Cui, F.; Ross, M. B.; Kim, D.; Sun, Y.; Yang, P. Structure-Sensitive CO<sub>2</sub> Electroreduction to Hydrocarbons on Ultrathin 5-fold Twinned Copper Nanowires. *Nano Lett.* **2017**, *17*(2), 1312-1317. DOI: 10.1021/acs.nanolett.6b05287
28. Suen, N. T.; Kong, Z. R.; Hsu, C. S.; Chen, H. C.; Tung, C. W.; Lu, Y. R.; Dong, C. L.; Shen, C. C.; Chung, J. C.; Chen, H. M. Morphology Manipulation of Copper Nanocrystals and Product Selectivity in the Electrocatalytic Reduction of Carbon Dioxide. *ACS Catal.* **2019**, *9*(6), 5217-5222. DOI: 10.1021/acscatal.9b00790

29. De Gregorio, G. L.; Burdyny, T.; Loiudice, A.; Iyengar, P.; Smith, W. A.; Buonsanti, R. Facet-Dependent Selectivity of Cu Catalysts in Electrochemical CO<sub>2</sub> Reduction at Commercially Viable Current Densities. *ACS Catal.* **2019**, *10*(9), 4854-4862. DOI: 10.1021/acscatal.0c00297
30. Mangione, G.; Huang, J.; Buonsanti, R.; Corminboeuf, C. Dual-Facet Mechanism in Copper Nanocubes for Electrochemical CO<sub>2</sub> Reduction into Ethylene. *J. Phys. Chem. Lett.* **2019**, *10*(15), 4259-4265. DOI: 10.1021/acs.jpcclett.9b01471
31. Bagger, A.; Ju, W.; Varela, A. S.; Strasser, P.; Rossmeisl, J. Electrochemical CO<sub>2</sub> Reduction: Classifying Cu Facets. *ACS Catal.* **2019**, *9*(9), 7894-7899. DOI: 10.1021/acscatal.9b01899
32. Van Hove, M. A.; Somorjai, G. A. A New Microfacet Notation for High-Miller-Index Surfaces of Cubic Materials with Terrace, Step and Kink Structures. *Surf. Sci.* **1980**, *92*(2-3), 489-518. DOI: 10.1016/0039-6028(80)90219-8
33. Tran, K.; Ulissi, Z. W. Active Learning Across Intermetallics to Guide Discovery of Electrocatalysts for CO<sub>2</sub> Reduction and H<sub>2</sub> Evolution. *Nat. Catal.* **2018**, *1*(9), 696-703. DOI: 10.1038/s41929-018-0142-1
34. Ulissi, Z. W.; Tang, M. T.; Xiao, J.; Liu, X.; Torelli, D. A.; Karamad, M.; Cummins, K.; Hahn, C.; Lewis, N. S.; Jaramillo, T. F.; et al. Machine-Learning Methods Enable Exhaustive Searches for Active Bimetallic Facets and Reveal Active Site Motifs for CO<sub>2</sub> Reduction. *ACS Catal.* **2017**, *7*(10), 6600-6608. DOI: 10.1021/acscatal.7b01648
35. Ma, S.; Sadakiyo, M.; Heima, M.; Luo, R.; Haasch, R. T.; Gold, J. I.; Yamauchi, M.; Kenis, P. J. Electroreduction of Carbon Dioxide to Hydrocarbons Using Bimetallic Cu-Pd Catalysts with Different Mixing Patterns. *J. Am. Chem. Soc.* **2017**, *139*(1), 47-50. DOI: 10.1021/jacs.6b10740
36. Huang, J.; Mensi, M.; Oveisi, E.; Mantella, V.; Buonsanti, R. Structural Sensitivities in Bimetallic Catalysts for Electrochemical CO<sub>2</sub> Reduction Revealed by Ag-Cu Nanodimers. *J. Am. Chem. Soc.* **2019**, *141*(6), 2490-2499. DOI: 10.1021/jacs.8b12381
37. Varandili, S. B.; Stoian, D.; Vavra, J.; Rossi, K.; Pankhurst, J. R.; Guntern, Y. T.; López, N.; Buonsanti, R. Elucidating the Structure-Dependent Selectivity of CuZn towards Methane and Ethanol in CO<sub>2</sub> Electroreduction Using Tailored Cu/ZnO Precatalysts. *Chem. Sci.* **2021**, *12*(43), 14484-14493. DOI: 10.1039/D1SC04271H
38. Huang, Y.; Chen, Y.; Cheng, T.; Wang, L. W.; Goddard III, W. A. Identification of the Selective Sites for Electrochemical Reduction of CO to C<sub>2+</sub> Products on Copper Nanoparticles by Combining Reactive Force Fields, Density Functional Theory, and Machine Learning. *ACS Energy Lett.* **2018**, *3*(12), 2983-2988. DOI: 10.1021/acscatal.8b01933
39. Wang, Z.; Yuan, Q.; Shan, J.; Jiang, Z.; Xu, P.; Hu, Y.; Zhou, J.; Wu, L.; Niu, Z.; Sun, J.; et al. Highly Selective Electrocatalytic Reduction of CO<sub>2</sub> into Methane on Cu-Bi Nanoalloys. *J. Phys. Chem. Lett.* **2020**, *11*(17), 7261-7266. DOI: 10.1021/acs.jpcclett.0c01261
40. Xiao, C.; Lu, B. A.; Xue, P.; Tian, N.; Zhou, Z. Y.; Lin, X.; Lin, W. F.; Sun, S. G. High-Index-Facet- and High-Surface-Energy Nanocrystals of Metals and Metal Oxides as Highly Efficient Catalysts. *Joule* **2020**, *4*(12), 2562-2598. DOI: 10.1016/j.joule.2020.10.002.
41. Quan, Z.; Wang, Y.; Fang, J. High-Index Faceted Noble Metal Nanocrystals. *Acc. Chem. Res.* **2013**, *46*(2), 191-202. DOI: 10.1021/ar200293n
42. Buonsanti, R.; Milliron, D. J. Chemistry of Doped Colloidal Nanocrystals. *Chem. Mater.* **2013**, *25*(8), 1305-1317. DOI: 10.1021/cm304104m
43. Lees, E. W.; Mowbray, B. A.; Parlane, F. G.; Berlinguette, C. P. Gas Diffusion Electrodes and Membranes for CO<sub>2</sub> Reduction Electrolysers. *Nat. Rev. Mater.* **2021**. DOI: 10.1038/s41578-021-00356-2

44. Jeon, H. S.; Timoshenko, J.; Rettenmaier, C.; Herzog, A.; Yoon, A.; Chee, S. W.; Oener, S.; Hejral, U.; Haase, F. T.; Roldan Cuenya, B. Selectivity Control of Cu Nanocrystals in a Gas-Fed Flow Cell through CO<sub>2</sub> Pulsed Electroreduction. *J. Am. Chem. Soc.* **2021**, *143*(19), 7578-7587. DOI: 10.1021/jacs.1c03443
45. Monteiro, M. C.; Dattila, F.; Hagedoorn, B.; García-Muelas, R.; López, N.; Koper, M. Absence of CO<sub>2</sub> Electroreduction on Copper, Gold and Silver Electrodes Without Metal Cations in Solution. *Nat. Catal.* **2021**, *4*(8), 654-662. DOI: 10.1038/s41929-021-00655-5
46. Yang, K.; Li, M.; Subramanian, S.; Blommaert, M. A.; Smith, W. A.; Burdyny, T. (2021). Cation-Driven Increases of CO<sub>2</sub> Utilization in a Bipolar Membrane Electrode Assembly for CO<sub>2</sub> Electrolysis. *ACS Energy Lett.* **2021**, *6*(12), 4291-4298. DOI: 10.1021/acsenerylett.1c02058
47. Liu, X.; Schlexer, P.; Xiao, J.; Ji, Y.; Wang, L.; Sandberg, R. B.; Tang, M.; Brown, K. S.; Peng, H.; Ringe, S.; et al. pH Effects on the Electrochemical Reduction of CO<sub>2</sub> towards C<sub>2</sub> Products on Stepped Copper. *Nat. Commun.* **2019**, *10*(1), 32. DOI: 10.1038/s41467-018-07970-9